Int. J. Electrochem. Sci., 8 **(2013)** 2791 - 2805

International Journal of
ELECTROCHEMICAL
SCIENCE
www.electrochemsci.org

Corrosion and Electrochemical Behavior of $Ni_{51}Fe_{22-x}Ga_{27}Ti_x$ Magnetic Shape Memory Alloys in 0.1 M NaCl Solution at Different Temperatures

Mohammed A. Amin[1,2,*], *Nader El-Bagoury*[1,3], *H. Shokry*[4,5]

[1] Materials and Corrosion Lab, Chemistry Department, Faculty of Science, Taif University, 888 Hawiya, Saudia Arabia
[2] Chemistry Department, Faculty of Science, Ain Shams University, P.O. Box 11566, Abbassia, Cairo, Egypt.
[3] Casting Technology Lab., Manufacturing Technology Dept., Central Metallurgical Research and Development Institute, CMRDI, P. O. Box 87 Helwan, Cairo, Egypt.
[4] Chemistry Department, Faculty of Applied Science, Umm-Al Qura University, Makkah, Saudia Arabia
[5] Chemistry Department, Faculty of Science, Kafr El-Sheikh University, Kafr El-Sheikh 33516, Egypt
[*]E-mail: maaismail@yahoo.com

Received: 28 November 2012 / *Accepted:* 9 January 2013 / *Published:* 1 February 2013

The effect of Ti addition, as an alloying element, and solution temperature (10-70 ^{o}C) on the pitting behavior of $Ni_{51}Fe_{22-x}Ga_{27}Ti_x$ (x = 0, 2, and 4%) magnetic shape memory alloys (MSMAs) has been studied in 0.1 M NaCl solution. Potentiodynamic anodic polarization and cyclic voltammetry were the electrochemical techniques used during pitting investigations, complemented with SEM/EDS examinations. From the obtained results it is inferred that the pitting potential (E_{pit}) and the repassivation potential (E_{rp}) are shifted to more negative (active) values with increasing temperature, corresponding to increased susceptibility towards the aggressive pitting attack of Cl^- anions. At a particular temperature and Cl^- concentration, the values of E_{pit} and E_{rp} shift to more noble potentials with increase in alloyed Ti content, referring to improved pitting corrosion resistance. Morphological studies using SEM came to the same conclusion and showed that the ratio of pitted area to total surface area (*i.e.*, pit area density) on the alloy surface decreased with alloyed Ti, while it increased with increase in temperature. The results of this study exemplify the specific role that solution temperature and alloyed Ti play in influencing the pitting mode of $Ni_{51}Fe_{22-x}Ga_{27}Ti_x$ MSMAs in a 0.1 M Cl^- neutral medium. It has been established that alloying $Ni_{51}Fe_{22}Ga_{27}$ MSMA with Ti (at the expense of Fe), particularly at low temperatures, is the condition most suitable for such alloys to resist initiation and propagation of pitting.

Keywords: Magnetic shape memory alloys; Pitting corrosion; Alloyed Ti; Solution temperature; SEM

1. INTRODUCTION

Shape memory alloys (SMAs) belong to a group of functional, smart materials with the unique property of ‘‘remembering” the shape they had before pseudoplastic deformation. Such an effect is based on crystallographic reversible thermo-elastic martensitic transformation. Due to these characteristics and super elasticity, SMAs, especially those of Ni and Ti, have attracted considerable attention as materials for medical devices such as guide wires, stents, filters, catheters, implants and others [1–3].

Magnetic shape memory alloys (MSMA) are a new class of materials, for which a strain of up to ~10% can be achieved by application of an external magnetic field [4]. Since the discovery of this effect in the Ni–Mn–Ga system [5,6], which is based on twin boundary motion in ferromagnetic martensite phases, these materials have generated a great research interest. A variety of applications for MSMA utilizing their actuator function are proposed, e.g. for micro-system devices [7], deformation sensors [8] or vibration damping [9].

It has been shown that MSMA experience a large change of shape under application conditions; the main reason why corrosion protection by additional coatings is impossible [10]. Therefore, the MSMA must exhibit a high ‘‘intrinsic” resistance against corrosion attack and a high surface self-healing ability [10]. However, and to our knowledge, little seems to be published concerning corrosion studies of such materials [10,11–13].

Therefore the objective of the present work is to investigate the effect of Ti addition (2% and 4%), as an alloying element at the expense of Fe, as well as solution temperature (10-70 ^{o}C) on passivity and passivity breakdown of $Ni_{51}Fe_{22}Ga_{27}$ MSMA in 0.1 M NaCl solution. Measurements were conducted based on potentiodynamic anodic polarization and cyclic voltammetry techniques, complemented with SEM/EDS examinations. Morphologies of the passivated and pitted surfaces were also studied as a function of alloy composition at 30 ^{o}C and 50 ^{o}C.

2. EXPERIMENTAL

The working electrodes employed in the present work are polycrystalline $Ni_{51}Fe_{22}Ga_{27}Ti_{0}$, $Ni_{51}Fe_{20}Ga_{27}Ti_{2}$ and $Ni_{51}Fe_{18}Ga_{27}Ti_{4}$ magnetic shape memory alloys. These alloys were made by using arc-melting under argon atmosphere (purity of elements is higher than 99.99%). The alloys were melted four times to ensure homogeneity and cast into a cylindrical copper mold set at the bottom of the furnace to prepare a rod with diameter of 10 mm and height of 70 mm.

These alloys were cast as cylindrical rods for the employed electrochemical technique. These rods machined carefully and mounted in polyester resin after the electric contact, with special care taken to prevent the presence of crevices. The exposed area was ~ 0.8 cm^2. Before each run, the samples were wet ground with 600-grit silicon carbide (SiC) paper and finally washed in distilled water, followed by immediate rinsing with absolute ethanol.

Electrochemical experiments were carried out in 0.1 M NaCl solution, as the corrosive medium (test solution), prepared with analytical grade chemicals and doubly distilled water. The test solution

was naturally aerated and its temperature was set up at various temperatures, namely 10, 20, 30, 40, 50, 60, and 70 ^{o}C using a temperature control water bath.

The experiments were performed in a 100 mL volume Pyrex glass cell using Pt wire as the auxiliary electrode. A silver/silver chloride (Ag/AgCl) reference electrode was used as a reference electrode, to which all potentials are referred.

The electrochemical cell was connected to a potentiostat; Autolab frequency response analyzer (FRA) coupled to an Autolab Potentiostat/Galvanostat (PGSTAT30) with FRA2 module connected to a personal computer.

The potentiodynamic anodic polarization curves were recorded by changing the electrode potential, automatically from -1.0 V (Ag/AgCl) to the required anodic potential at a potential scan rate of 1.0 mV s^{-1}. Cyclic voltammetric measurements were carried out by sweeping linearly the potential from the starting potential (-1.0 V) into the positive direction at 1.0 mV s^{-1} scan rate till a required potential value, and then reversed with the same scan rate till the starting potential to form one complete cycle.

Before each run, the open circuit potential of the working electrode was measured as a function of time during 2h; the time necessary to reach a quasi-stationary value for the open circuit potential. At least three separate experiments were carried out for each run to ensure reproducibility of results. The reproducibility of the polarization curves was good. Values of the corrosion potential (E_{corr}), the pitting potential (E_{pit}) and the repassivation potential (E_{rp}) were reproducible to about ± 15-25 mV(Ag/AgCl). This good reproducibility was expected since a protracted immersion period (2h) was undertaken to achieve a steady corrosion potential.

Morphologies and composition of the passivated and pitted surfaces of the three tested MSMAs were examined in 0.1 M NaCl solutions as a function of the percentage of the alloyed Ti (0, 2, and 4%) at 30 ^{o}C and 50 ^{o}C, using an Analytical Scanning Electron Microscope JEOL JSM 6390 LA.

For each experiment, the electrode was immersed for 5 min in 0.1M NaCl at a given temperature under potentiostatic regime at a fixed anodic potential, E_a, (where $E_a > E_{pit}$ for any of the three tested alloys), and finally washed thoroughly and submitted to 20 min of ultrasonic cleaning in order to remove loosely adsorbed ions.

3. RESULTS AND DISCUSSION

3.1. Cyclic polarization behavior of $Ni_{51}Fe_{22}Ga_{27}$ magnetic shape memory alloys in 0.1 M NaCl

Figure 1 presents a typical cyclic polarization curve recorded for $Ni_{51}Fe_{22}Ga_{27}Ti_0$ MSMA between −1.0V and 1.0V (Ag/AgCl) in 0.1 M NaCl solution at a scan rate of 1.0 mV s^{-1} at 30 ^{o}C. Similar results, as will be shown later, are obtained for the other tested MSMAs, which alloyed with Ti at the expense of Fe, namely $Ni_{51}Fe_{20}Ga_{27}Ti_2$ and $Ni_{51}Fe_{18}Ga_{27}Ti_4$ alloys.

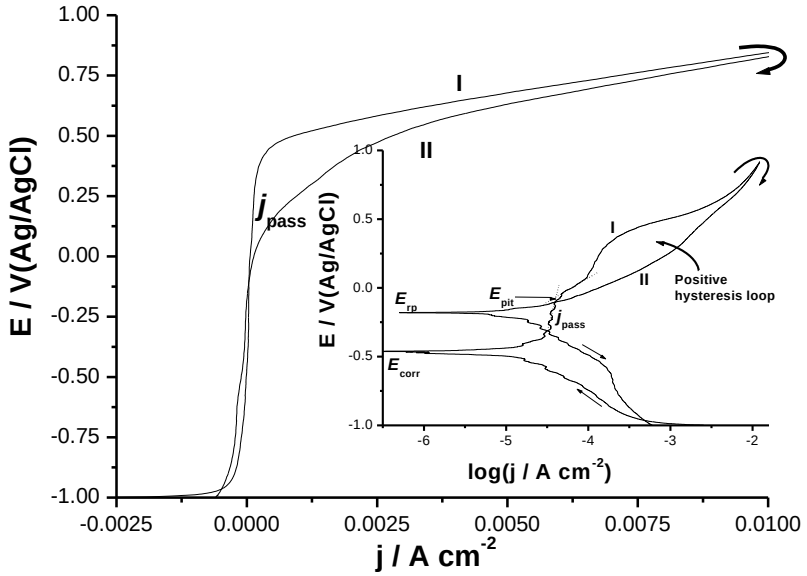

Figure 1. Cyclic polarization (*E* vs. *j*) curve recorded for $Ni_{51}Fe_{22}Ga_{27}Ti_0$ MSMA in 0.1 M NaCl solution at a scan rate of 1.0 mV s^{-1} at 25 ^{o}C – Insert: same polarization plot, but in its corresponding logarithmic scale (*E* vs. log *j*).

On positive going scan, the cathodic current density decreases gradually and reaches a zero value at the corrosion potential (E_{corr}). The anodic excursion span does not exhibit active dissolution region near E_{corr} due to passivation of the electrode surface.

Passivity, and hence the corrosion resistance, of such alloys may rely on the presence of oxide films of Ni, Fe, Ga, and Ti, on their surfaces. The chemical composition of such oxides is expected to be similar to that of the oxides presented in the work of Gebert et. al [10]. However, work is currently ongoing in a complementary paper to investigate and analyze the effect of Ti addition on the microstructure and chemical composition of the passive oxide films, based on XRD and XPS examinations.

Referring again to the work of Gebert et. al [10], they studied the corrosion and passivation behaviour of bulk polycrystalline martensite $Ni_{50}Mn_{30}Ga_{20}$ and austenite $Ni_{48}Mn_{30}Ga_{22}$ magnetic shape memory alloys in electrolytes with different pH values. Linear anodic and cyclic potentiodynamic polarisation methods and anodic current transient measurements were used in their nice study, complemented with SEM and XPS examinations. The work of Gebert et. al revealed that the passive films formed in near neutral media (pH 5–8.4) are composed of $Ni(OH)_2$, NiOOH and Ga_2O_3 in the outer region and of NiO, MnO_2 and MnO in the metal-near region.

Generally, the passive oxide layer serves two purposes [14]: (i) It increases the stability of the surface layer by protecting the bulk material from corrosion; and (ii) It creates a physical and chemical barrier against the oxidation of the base alloying elements, namely Ni and Fe, by modifying their oxidation pathways [15].

However, the recorded polarization curve is characterized by a small passive region, as shown in the insert of Fig. 1. This narrow passive region reflects without any doubt the severity nature of the pitting attack induced by Cl^- anions.

The end of this narrow passive region denotes the pitting potential, E_{pit}, above which the passive film breaks down and pits initiate on the alloy surface. This is indicated by the rapid increase in the passive current (j_{pass}), without any sign for oxygen evolution, as a consequence of the passivity breakdown, see region I. The extension (wideness) of the passive region is found to be a function of alloy composition, see later.

Initiation of pitting could be ascribed to adsorption of Cl^- anions on the oxide/solution interface under the influence of electric field in competition with the passive layer forming species for active surface sites on the oxide [16]. Such adsorption of Cl^- anions is confirmed from the EDS spectra (not included here). In the present work, EDS survey spectra were recorded for specimens of the three tested alloys exposed for 5.0 min in 0.1 M NaCl under potentiostatic regime at a fixed anodic potential, E_a, (where $E_a > E_{pit}$ for any of the three tested alloys).

The obtained EDS spectra indicated that the passivated and corroded surfaces of the three tested alloys at all locations (even inside pits) had the elemental composition Ni, Fe, Ga, Ti, O and Cl. The atomic percentage of each element depends on the composition of each tested alloy. The Cl signal is due undoubtedly to Cl^- anions. It seems therefore that the formed protective oxide films contain a certain amount of incorporated Cl^- anions.

Adsorption of Cl^- anions is followed by passivity breakdown and initiation of pits, based on the point defect model (PDM) developed by Macdonald and co-workers [17], see later.

Also, microscopic examinations revealed, as will be seen later and fully discussed in section 3.6, passivity breakdown of the tested alloys followed by initiation and propagation of pits to an extent depending on Ti content in the tested MSMA.

Based on the above arguments, the anodic current passing through our narrow passive region (termed the passive current, j_{pass}) may therefore correspond to the replacement of chemically dissolved oxide by the adsorbed Cl^- anions, resulting in the formation of a less protective (thin and/or porous) passive film.

The adsorption of Cl^- seems to enhance with anodic potential. This is clearly seen from the increase in j_{pass} with potential within the narrow passive region (inspect again the insert of Fig. 1). This increase in j_{pass} with potential continues till E_{pit} is reached. When the applied potential exceeds E_{pit}, as previously mentioned, j_{pass} remarkably increases denoting passivity breakdown, initiation and propagation of pitting attack.

3.2. Mechanism of passivity breakdown and initiation and growth of stable pits

Following Frankel [18], passivity breakdown is a rare occurrence that happens extremely rapidly on a very small scale, making direct observation extraordinarily difficult.

The passive film is often drawn schematically as a simple inert layer covering the underlying metal and blocking access of the environment to the metal [18]. As reported by Frankel [18], the

reality is much more complicated. Depending on alloy composition, environment, potential, exposure history, and other factors, this film can have a range of thickness, structure, composition, and protectiveness [18]. The passage of a finite passive current density is evidence of continual reaction of the metal to result in film thickening, dissolution into the environment, or some combination of the two [18].

Theories for passive film breakdown and pit initiation, considering pure metal systems, have been categorized in three main mechanisms that focus on passive film penetration, film breaking, or adsorption [19]. Different mechanisms or combinations of these mechanisms may be valid for different metal/environmental systems.

The point-defect model (PDM) developed by Macdonald and coworkers is employed to describe passive film growth by the movement of point defects under the influence of an electrostatic field [20]. The major point defects in an oxide film are assumed to be electrons, holes, and metal and oxide vacancies. Transport of vacancies across the film controls the film growth according to this view.

The point-defect model has been used to explain pit initiation by assuming that aggressive ion (chloride) adsorption and incorporation at the outer surface of the barrier oxide layer results in the formation of cationic vacancies [17]. These vacancies diffuse to the metal/oxide surface where they are annihilated by the oxidative injection of cations from the metal. However, if the flux of vacancies is larger than can be accommodated by oxidation, the vacancies will condense at the metal/film interface to form a void that is the first step in the pitting process according to this model.

After being initiated, pit growth takes place immediately as a result of increasing the concentration of the aggressive anions by migration [21]. The increased concentration of metal cations inside the pit leads to changes in localized solution chemistry. First, following Galvele [22], hydrolysis occurs to lower the pH. A second effect arises from the well-recognized requirement that electrical neutrality must be maintained throughout the electrolyte.

Therefore, the aggressive Cl^- anions must migrate into the pit to compensate the local increase in metal cations concentration, as shown by the theoretical analysis of Ateya and Pickering [23]. This reflects the auto-catalytic nature of the pitting corrosion process. This leads to a greater imbalance between the film forming reactions and the dissolution reactions.

Consequently, the pit once initiated continues to propagate and enlarge (*i.e.*, enhances in size and depth). This is quite evident from the sudden increase in the passive current (j_{pass}) at potentials exceeding E_{pit}, as represented by region I in Fig. 1.

3.3. Effect of reversing the potential scan

Upon reversing the potential sweep, the reverse (pitting) current exhibits a positive hysteresis loop (see Fig. 1 and its insert), characteristic of pitting corrosion phenomena [24-32]. This means that pitting continues even after scan reversal, because the pitting attack is enhanced after the pit initiation (autocatalytic character of pitting) [33].

Generally, the existence of a hysteresis loop in a cyclic potentiodynamic polarization curve indicates a delay in repassivation of an existing pit when the potential is scanned toward negative direction. The larger the hysteresis loop, the more difficult it becomes to repassivate the pit [33].

The pitting current in the reverse scan decreases and completely suppressed at a certain potential known as the repassivation potential (E_{rp}) [34], where pit growth is arrested (see region II in Fig. 1).

The location of E_{rp} with respect to E_{corr} is well-defined in the E vs. log j plot, as shown in the insert of Fig. 1. In the present work, E_{rp} is defined as the potential on the reverse scan at which the anodic current becomes zero (i.e., the current changes polarity in the logarithmic scale [35]); inspect again the insert of Fig. 1. Determination of E_{rp} is essential in order to establish the passive and pitting potential regions of the system.

Indeed in pitting corrosion studies, E_{rp} can be considered as a very important pitting corrosion parameter besides the well-known relevant potential in localized corrosion studies, i.e., E_{pit}. At potentials more negative than E_{rp}, the electrode is protected by an oxide film and pitting will only take place at more positive potentials [33].

Further inspection of the current hysteresis loop, together with the location of E_{rp} with respect to E_{corr}, reveals that the tested alloy was able to repassivate easily after passivity breakdown. This is because E_{rp} locates inside the passive region (i.e., more anodic than E_{corr}). This is in contrary to our previously published work concerning pitting corrosion studies of Al in gluconic acid solutions [30]. Al suffered severe pitting in gluconic acid solutions, and found it difficult to repassivate since its E_{rp} located outside the passive region [30].

It is worthy noting that the reverse cathodic sweep, after the hysteresis loop has been completed, does not involve any cathodic peaks. This strongly suggests that the pitting corrosion products are strongly adhered to the surface and not easy to reduce. Or, it is probable that, the current associated with the cathodic process (i.e., reduction) of the pitting corrosion products is very small so that the reduction process is associated with the surface confined to surface-confined species reduction conversions.

It is also noted that the reverse cathodic current density is higher than the forward cathodic current density (inspect again the insert of Fig. 1). The difference between the two cathodic currents can be due to the reduction of the remaining oxide film on the electrode surface.

It seems that the reduction process of the pitting corrosion products of this system can be very complicated, in which different pitting corrosion product species could be involved. Furthermore, along with the redox reactions, local pH changes of the electrode surface are expected, particularly when the bulk electrolyte is not buffered and the solution is not agitated, as in the current case. As a result, any further interpretation based only on CV data would be unwise. This point therefore deserves further investigations in our future studies, in which additional measurements, using for example, ring-disk electrodes, will be performed in order to follow the release of such species.

3.4. Effect of Ti addition on the cyclic polarization behavior of $Ni_{51}Fe_{22}Ga_{27}$ alloy in 0.1 M NaCl

Figure 2 illustrates the effect of Ti addition (2% and 4%), as an alloying element at the expense of Fe, on the cyclic polarization behavior of $Ni_{51}Fe_{22}Ga_{27}$ MSMAs in 0.1 M NaCl solution at a scan rate of 1.0 mV s^{-1} at 30 ^{o}C.

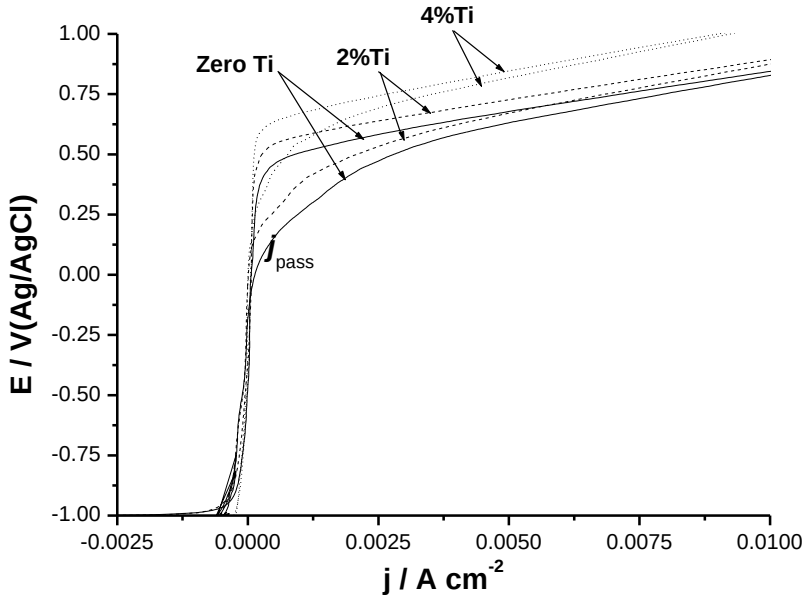

Figure 2. Cyclic polarization curves recorded for $Ni_{51}Fe_{22-x}Ga_{27}Ti_x$ MSMAs (x = 0, 2, and 4%Ti) in 0.1 M NaCl solution at a scan rate of 1.0 mV s^{-1} at 30 ^{o}C.

It is seen in all cases that the electrode retains its passivity up to the pitting potential (E_{pit}) at which the passive current (j_{pass}) rises abruptly revealing passivity breakdown, followed by initiation and propagation of pits. It follows from Fig. 2 that the extension of the passive region, E_{pit}, E_{rp}, and the charge consumed during hysteresis loop formation (i.e., how wide the hysteresis loop is?) vary depending on %Ti in the tested alloy.

Both E_{pit} and E_{rp} shift in the noble direction and the hysteresis loop gets narrower upon alloying $Ni_{51}Fe_{22}Ga_{27}$ with Ti. These events are more significant in presence of 4%Ti than in presence of 2%Ti. These findings reveal that the magnetic shape memory alloy $Ni_{51}Fe_{22}Ga_{27}$, when alloyed with Ti, finds it difficult to pit. In addition the pit once initiated, repassivates easily; a narrow hysteresis loop is developed. This corresponds to improved pitting corrosion resistance, upon alloying it with Ti.

Similar results were previously obtained in our lab [36]; where both meta-stable and stable pitting events on the surface of pure Al and three Al–Si alloys, namely (Al + 6%Si), (Al + 12%Si) and (Al + 18%Si) alloys, were investigated in deaerated neutral $NaClO_4$ solutions of various concentrations. Alloyed Si was also found to significantly enhance the pitting corrosion resistance of Al to an extent depending upon its content in the tested alloy [36].

In the current study, the role played by the alloyed Ti in improving the pitting corrosion resistance of $Ni_{51}Fe_{22}Ga_{27}$ MSMA in NaCl solutions can be explained on the basis of our previous

study [36]. In this respect, any localized dissolution will preferentially dissolve Ni and Fe (qualitatively detected in the test solution after the corrosion experiment has been completed). The preferential dissolution of Ni and Fe will leave the surface enriched in unreactive Ti atoms.

Enrichment of alloy surface in unreactive Ti atoms during dissolution blocks the active sites available for Ni and Fe dissolution. At this stage, dissolution is retarded and pitting ceases. In order for pitting to recommence, the potential must be raised even higher [to $(E_{pit})_{alloy}$] to activate dissolution at the less favourable sites.

As the alloyed Ti content is increased from 2% to 4%, Ti atoms will appear with greater frequency. Therefore, dissolution processes will be retarded until increasingly higher potentials are reached. Therefore, $(E_{pit})_{alloy}$ must increase with Ti content, Fig. 2.

It is also possible that the alloyed Ti atoms incorporate in the passive oxide films, repairing defects. Thus, the dissolution of the passive oxide film ceases. This makes it more difficult for Cl^- anions to migrate through the oxide film. The alloyed Ti would as a result increase the difficulty of soluble film formation required for film rupture to occur [37].

Alloyed Ti atoms may also slow down the rate of metal dissolution by reducing the amount of free metal ions in the pit solution resulting in a decrease in diffusion of Cl^- into the pit and reduction in diffusion of metal cations out of the pit [38].

3.5. Effect of temperature on the anodic behavior of alloy $Ni_{51}Fe_{22}Ga_{27}$ in 0.1 M NaCl

Figures 3-5 show the effect of solution temperature (10-70 ^oC) on the potentiodynamic anodic polarization responses of the three tested MSMAs in 0.1 M NaCl solution at a scan rate of 1.0 mV s^{-1}.

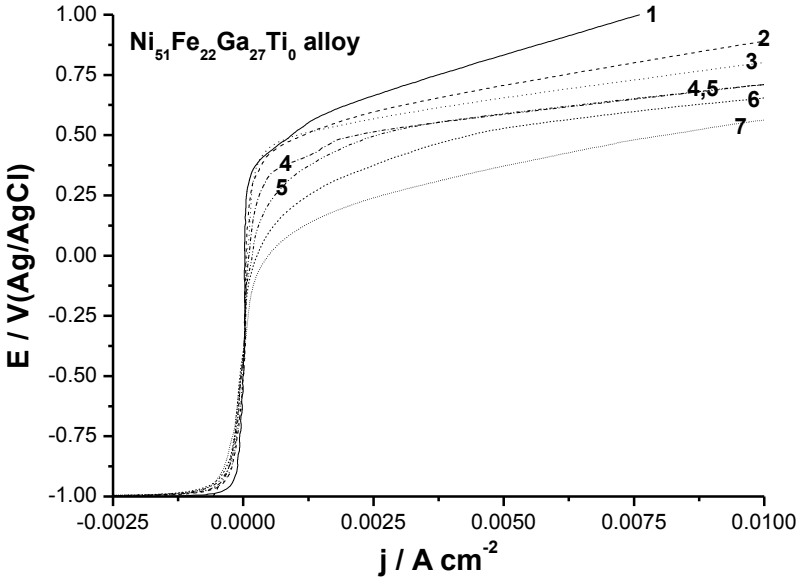

Figure 3. Potentiodynamic anodic polarization curves recorded for $Ni_{51}Fe_{22}Ga_{27}Ti_0$ MSMA in 0.1 M NaCl solution at a scan rate of 1.0 mV s^{-1} and at different temperatures (10-70 ^oC). (1)10 ^oC; (2) 20 ^oC; (3) 30 ^oC; (4) 40 ^oC; (5) 50 ^oC; (6) 60 ^oC; (7) 70 ^oC.

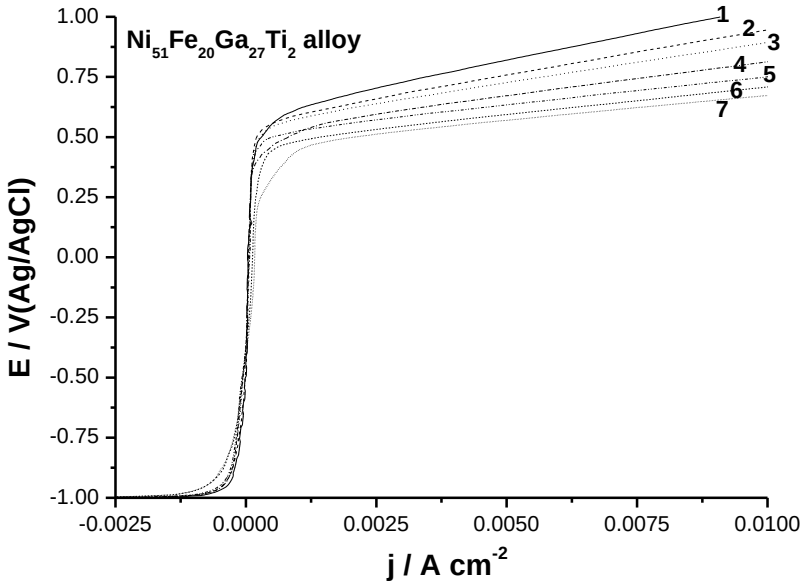

Figure 4. Potentiodynamic anodic polarization curves recorded for $Ni_{51}Fe_{20}Ga_{27}Ti_2$ MSMA in 0.1 M NaCl solution at a scan rate of 1.0 mV s^{-1} and at different temperatures (10-70 ^{o}C). (1)10 ^{o}C; (2) 20 ^{o}C; (3) 30 ^{o}C; (4) 40 ^{o}C; (5) 50 ^{o}C; (6) 60 ^{o}C; (7) 70 ^{o}C.

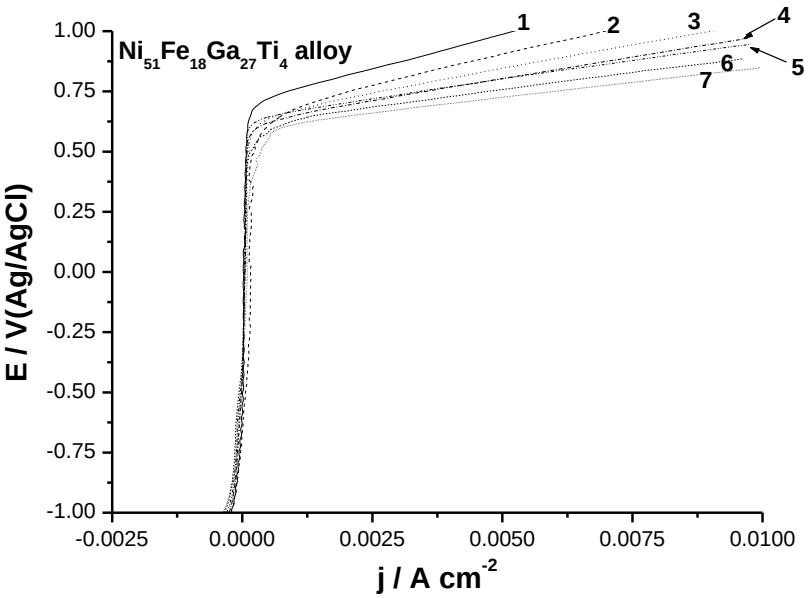

Figure 5. Potentiodynamic anodic polarization curves recorded for $Ni_{51}Fe_{18}Ga_{27}Ti_4$ MSMA in 0.1 M NaCl solution at a scan rate of 1.0 mV s^{-1} and at different temperatures (10-70 ^{o}C). (1)10 ^{o}C; (2) 20 ^{o}C; (3) 30 ^{o}C; (4) 40 ^{o}C; (5) 50 ^{o}C; (6) 60 ^{o}C; (7) 70 ^{o}C.

A negative shift in E_{pit} is noticed for the all tested alloys with increasing temperature, corresponding to increased susceptibility to pitting. The values of E_{pit}, at any given temperature, are always higher for the MSMA that is alloyed with the highest Ti content, 4%Ti, (i.e., $Ni_{51}Fe_{18}Ga_{27}Ti_4$ alloy), confirming its highest pitting corrosion resistance among the tested alloys.

The relation between E_{pit} and T for the three tested samples is given in Fig. 6. This relation approaches a linear relationship with temperature coefficients of -0.00918 VK^{-1}, -0.00402 VK^{-1}, and -0.0027 VK^{-1} for $Ni_{51}Fe_{22}Ga_{27}Ti_0$, $Ni_{51}Fe_{20}Ga_{27}Ti_2$, and $Ni_{51}Fe_{18}Ga_{27}Ti_4$ alloys, respectively.

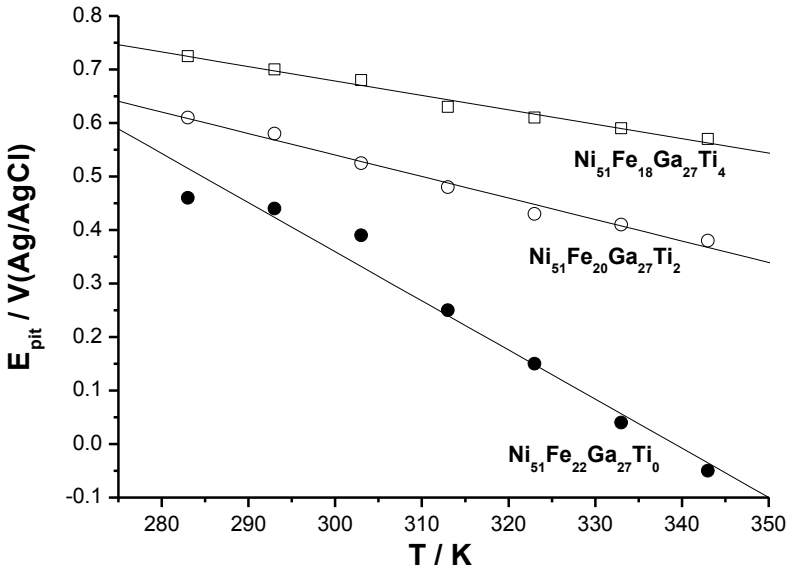

Figure 6. Variation of E_{pit} of the three tested alloys with solution temperature (10-70 ^oC) in 0.1 M NaCl solutions.

The low temperature coefficient recorded for $Ni_{51}Fe_{18}Ga_{27}Ti_4$ alloy (-0.0027 VK^{-1}) indicates that the rise of temperature has a little acceleration influence on pit initiation, certainly because of the high content of the alloyed Ti (4%) that exists in this alloy.

On the other hand, the increase in the slope of the *j vs. E* plots following E_{pit} with temperature (Figs. 3.5) reveals that increasing temperature has an accelerating influence on pit propagation. These findings imply that increasing solution temperature is destructive to passivity of the tested SMAs, but to an extent depending on their chemical composition (%Ti in the tested alloy). This leads to the occurrence of pitting corrosion, the severity of which was found to decrease with Ti content (see later).

Such accelerating influence of solution temperature on the pitting corrosion process can be explained on the basis that an increase in temperature accelerates the rates of migration and diffusion of the reactant and product species into and from pits. In addition, an increase in temperature enhances the solubility of the passive oxide film [39], which in turn may increase its porosity [40].

The increase in the porosity of the passive oxide film with increase in temperature may create new active sites for the aggressive Cl^- anions to be adsorbed. This may account for the increased adsorption of Cl^- with temperature, as evidenced from EDS analyses of the present work, which revealed increased adsorption of Cl^- anions in the passive film and inside pits with solution temperature. Similar findings were obtained in our previous studies during pitting corrosion of Al induced by SCN^- anions [28], and Zn by the aggressive $S_2O_3^{2-}$ anions [32]. Augustynski et al. [41],

using XPS method, came to the same conclusion. He also observed an increased adsorption of Cl^- at high temperatures.

The increased adsorption of Cl^- anions with rise of temperature hindered the oxide film formation by competitive adsorption between oxygen containing (passivating) species and Cl^- anions, resulting in the decrease of the oxide film resistance [40]. This means that the oxide film formed high solution temperatures has lower degree of passivity compared with that formed at lower temperatures.

3.6. Pitting morphologies as a function of alloy composition and temperature

Figures 7a-7g are SEM images to show the morphologies of the pitted surfaces of $Ni_{51}Fe_{22}Ga_{27}Ti_0$, $Ni_{51}Fe_{20}Ga_{27}Ti_2$, and $Ni_{51}Fe_{18}Ga_{27}Ti_4$ alloys in 0.1 M NaCl solutions at 30 ^oC and 50 ^oC. Such morphologies are recorded after exposing the three tested alloys to the aggressive pitting attack of Cl^- anions under potentiostatic regime. Each alloy was held at a constant applied anodic potential, E_a, ($E_a > E_{pit}$ of any tested alloy) for 5.0 min.

No pitting has occurred on the surfaces of the tested alloys exposed to a potential negative to E_{pit} at 30 ^oC and 50 ^oC due to passivation; see for example image (a) recorded for $Ni_{51}Fe_{22}Ga_{27}Ti_0$ at 30 ^oC. Almost similar morphologies were obtained for the passivated surfaces of the other two tested alloys at 30 ^oC and 50 ^oC (such morphologies are not included here).

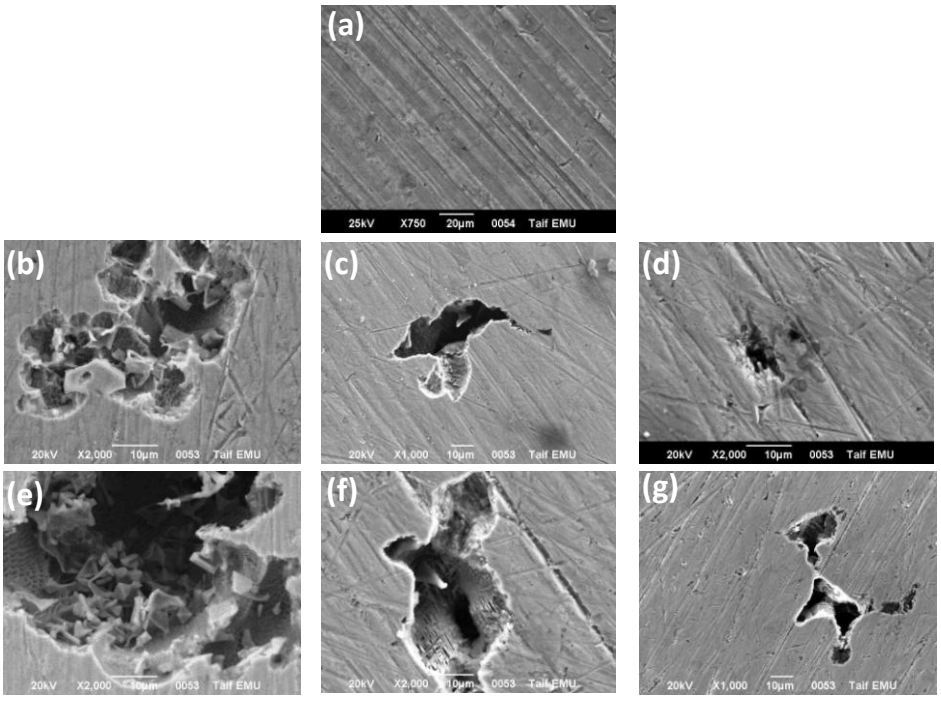

Figure 7. Morphologies of the (a) passive surface of $Ni_{51}Fe_{22}Ga_{27}Ti_0$ alloy at 30 ^oC and the (b-g) pitted surfaces of (b,e) $Ni_{51}Fe_{22}Ga_{27}Ti_0$, (c,f) $Ni_{51}Fe_{20}Ga_{27}Ti_2$, and (d,g) $Ni_{51}Fe_{18}Ga_{27}Ti_4$ alloys in 0.1 M NaCl solutions at 30 ^oC (images b-d) and 50 ^oC (images e-g). Such morphologies are recorded after exposing the three tested alloys to the aggressive pitting attack of Cl^- anions under potentiostatic regime. Each alloy was held at a constant applied anodic potential, E_a, ($E_a > E_{pit}$ of any tested alloy) for 5.0 min.

On the other hand, the electrodes that are polarized at a fixed anodic potential beyond E_{pit}, suffered from pitting attack (images b-g), the intensity of which varies according to solution temperature and chemical composition of each tested alloy. In all cases, the formed pits are surrounded on all sides by the regions covered with oxide layer and corrosion products that accumulate around the edges of pits. Similar morphologies were previously obtained in our lab during studying the effect of Re (as an alloying element) on the localized corrosion behavior of $Ti_{51}Ni_{49-x}Re_x$ (x = 0, 0.1, and 0.3%) shape memory alloys in KBr solutions [31].

Images b-g revealed that, at any given temperature, the pitted areas decrease when the percentage of alloyed Ti in the tested alloy increases from 2% to 4%. At a given chemical composition, the pitting attack is more severe at 50 ^{o}C (images e-g) than at 30 ^{o}C (images b-d). Or in other words, the areas of the protective oxide layer increase at the expense of the pitted ones with increase in alloyed Ti content, particularly at low temperatures.

This means that the ratio of pitted area to total surface area (*i.e.*, pit area density) decreased, corresponding to increased resistance against pitting, with solution temperature lowering and with increase in Ti content. Further inspection of Fig. 7 demonstrates that the severity of pitting attack is markedly suppressed in presence of 4%Ti, with no corrosion products. This confirms that the alloy $Ni_{51}Fe_{18}Ga_{27}Ti_4$ possesses, at any given temperature, the highest pitting corrosion resistance among the tested MSMAs.

4. CONCLUSION

Passivity and passivity breakdown, followed by initiation and growth of stable pits were studied on the surfaces of three magnetic shape memory alloys (MSMAs), namely $Ni_{51}Fe_{22}Ga_{27}Ti_0$, $Ni_{51}Fe_{20}Ga_{27}Ti_2$, and $Ni_{51}Fe_{18}Ga_{27}Ti_4$ in 0.1 M NaCl solution as a function of solution temperature (10-70 ^{o}C). Measurements were carried out by means of potentiodynamic anodic polarization and cyclic voltammetry techniques, complemented with SEM/EDS examinations. Results of the present work revealed the following conclusions:

(i) Alloying $Ni_{51}Fe_{22}Ga_{27}$ MSMA with Ti enhanced its pitting corrosion resistance, at a given temperature, to an extent proportionally to the percentage of the alloyed Ti in the tested MSMA. This is quite evident from the increase in the positive shift of the pitting potential (E_{pit}) and the repassivation potential (E_{rp}) with alloyed Ti content.

(ii) At any given chemical composition of the tested alloys, *i.e.*, at a fixed Ti content, the values of E_{pit} and E_{rp} are found to shift to more negative (active) potentials with increasing temperature, corresponding to increased susceptibility towards passivity breakdown and initiation and propagation of stable pits as a result of the aggressive attack of Cl^- anions.

(iii) Morphological studies using SEM examinations of the pitted surfaces revealed that, at any given alloyed Ti content, the pit area density (*i.e.*, the ratio of pitted area to total surface area) increases, and hence the pitting corrosion resistance decreases, with increasing solution temperature.

(iv) SEM images of the pitted surfaces also revealed that, at a given solution temperature, the severity of pitting corrosion is significantly suppressed when the percentage of the alloyed Ti increases in the tested MSMA from 2% to 4%.

ACKNOWLEDGEMENT
The authors acknowledge the financial aid received from Taif University, Saudia Arabia (Project No. 1/433/2097).

References

1. K. Otsuka, X. Ren, *Intermetallics*, 7 (1999) 511.
2. S. Miyazaki, Medical and dental applications of shape memory alloys, In: Otsuka K, Wayman C, editors. Shape memory materials. Cambridge: Cambridge University Press; 1998. p. 267–80.
3. T. Duerig, A. Pelton, D. Stockel, *Mater. Sci. Eng. A*, 273–275 (1999) 149.
4. A. Sozinov, A.A. Likhachev, N. Lanska, K. Ullakko, *Appl. Phys. Lett*., 80 (2002) 746.
5. V.A. Chernenko, E. Cesari, V.V. Kokorin, I.N. Vitenko, *Scripta Mater*., 33 (1995) 1239.
6. K. Ullako, J.K. Huang, C. Kantner, R.C. O'Handley, V.V. Kokorin, *Appl. Phys. Lett*., 69 (1996) 1966.
7. M. Kohl, D. Brugger, M. Ohtsuka, T. Takagi, *Sensors Actuators*, 114 (2004) 445.
8. N. Sarawate, M. Dapino, *Appl. Phys. Lett*., 88 (2006) 121923.
9. J. Feuchtwanger, K. Griffin, J.K. Juang, D. Bono, R.C. O'Handley, S.M. Allen, *J. Magn. Magn. Mater*., 272–276 (2004) 2038.
10. A. Gebert, S. Roth, S. Oswald, L. Schultz, *Corros. Sci*., 51 (2009) 1163.
11. X.W. Liu, O. S◌derberg, Y. Ge, A. Sozinov, V.K. Lindroos, *Mater. Sci. Forum*, 394–395 (2002) 565.
12. X.W. Liu, O. S◌derberg, Y. Ge, N. Lanska, K. Ullakko, V.K. Lindroos, *J. Phys. IV France*, 112 (2003) 935.
13. L.L. Stepan, D.S. Levi, E. Gans, K.P. Mohanchandra, M. Ujihara, G.P. Carman, *J. Biomed. Mater. Res*., 82 (2007) 768.
14. X.J. Yan, D.Z. Yang, X.P. Liu, *Materials Characterization*, 58 (2007) 623–628.
15. O. Cissé, O. Savadoga, M. Wu, L'H Yahia, *J. Biomed. Mater. Res.*, 61 (2002) 339.
16. L. Sziraki, A. Sziraki, I. Geroes, Z. Vertesy, and L. Kiss, *Electrochim. Acta*, 43 (1998) 175.
17. L. F. Lin, C. Y. Chao, and D. D. Macdonald, *J. Electrochem. Soc.*, 128 (1981) 1194.
18. G. S. Frankel, *J. Electrochem. Soc*., 145 (1998) 2186.
19. H.-H. Strehblow, in *Corrosion Mechanisms in Theory and Practice*, P. Marcus and J. Oudar, Editors, p. 201, Marcel Dekker, Inc., New York (1995).
20. C. Y. Chao, L. F. Lin, and D. D. Macdonald, *J. Electrochem. Soc.*, 128 (1981) 1187.
21. N.D. Budiansky, J.L. Hudson, J.R. Scully, *J. Electrochem. Soc*., 151 (2004) B233.
22. J.R. Galvele, in: R.P. Frankenthal, J. Kruger (Eds.), Passivity of Metals, The Electrochemical Society, Inc., Princeton, NJ, 1978, p. 285.
23. B.G. Ateya, H.W. Pickering, in: R.P. Frankenthal, J. Kruger (Eds.), Passivity of Metals, The Electrochemical Society, Inc., Princeton, NJ, 1978, p. 350.
24. M.A. Amin, *Electrochim. Acta*, 50 (2005) 1265.
25. M.A. Amin, S.S. Abd El Rehim, E.E.F. El Sherbini, *Electrochim. Acta*, 51 (2006) 4754.
26. M.A. Amin, S.S. Abd El Rehim, S.O. Moussa, A.S. Ellithy, *Electrochim. Acta*, 53 (2008) 5644.
27. M.A. Amin, H.H. Hassan, S.S. Abd El Rehim, *Electrochim. Acta*, 53 (2008) 2600.
28. M.A. Amin, S.S. Abd El-Rehim, E.E.F. El-Sherbini, S.R. Mahmoud, M.N. Abbas, *Electrochim. Acta*, 54 (2009) 4288.

29. M.A. Amin, S.S. Abd El Rehim, A.S. El-Lithy, *Electrochim. Acta*, 55 (2010) 5996.
30. M.A. Amin, S.S. Abd El Rehim, A.S. El-Lithy, *Corros. Sci*., 52 (2010) 3099.
31. M.A. Amin, N. El-Bagoury, A.A. Omar, A.S. Megahed, *Int. J. Electrochem. Sci.*, 7 (2012) 2643.
32. S. S. Abd El-Rehim, E.Hamed, A. M. Shaltot, M. A. Amin, *Z. Phys. Chem*., 226 (2012) 59-85.
33. H. Kaesche, *Werkt. Korros*., 39 (1988) 152.
34. Z. Szklarska-Smialowska, Pitting Corrosion of Metals, NACE, Houston, TX, 1986.
35. M. Finsgar, S. Fassbender, S. Hirth, I. Milosev, *Mater. Chem. Phys*., 116 (2009) 198.
36. M.A. Amin, H.H. Hassan, O.A. Hazzazi, M.M. Qhatani, *J Appl. Electrochem.*, 38 (2008) 1589.
37. R.T. Foley, *Corrosion*, 42 (1986) 277.
38. H. Bohni, *Langmiur*, 3 (1987) 924.
39. M. Elboujdaini and E. Ghali, *Corros. Sci*., 30 (1990) 855.
40. J.-J. Park and S.-I. Pyun, *Corros. Sci*. 45 (2003) 995.
41. J. Augustynski, R. P. Frankenthal, and J. Kruger (Eds.), Proceedings of the Fourth International Symposium on Passivity, The Electrochemical Society, Pennington, NJ, 1978, p. 997.